Fanni D. Sypaseuth, Emanuela Gallo, Serhat Çiftci and Bernhard Schartel*

Polylactic acid biocomposites: approaches to a completely green flame retarded polymer

DOI 10.1515/epoly-2017-0024
Received January 25, 2017; accepted May 8, 2017; previously published online June 20, 2017

Abstract: Basic paths towards fully green flame retarded kenaf fiber reinforced polylactic acid (K-PLA) biocomposites are compared. Multicomponent flame retardant systems are investigated using an amount of 20 wt% such as $Mg(OH)_2$ (MH), ammonium polyphosphate (APP) and expandable graphite (EG), and combinations with silicon dioxide or layered silicate (LS) nanofillers. Adding kenaf fibers and flame retardants increases the E modulus up to a factor 2, although no compatibilizer was used at all. Thus, in particular adding EG and MH decreases the strength at maximum elongation, and kenaf fibers, MH, and EG are crucial for reducing the elongation to break. The oxygen index is improved by up to 33 vol% compared to 17 vol% for K-PLA. The HB classification of K-PLA in the UL 94 test is outperformed. All flame retarded biocomposites show somewhat lower thermal stability and increased amounts of residue. MH decreases the fire load significantly, and the greatest reduction in peak heat release rate is obtained for K-PLA/15MH/5LS. Synergistic effects are observed between EG and APP (ratio 2:1) in flammability and fire properties. Synergistic multicomponent systems containing EG and APP, or MH with adjuvants offer a promising route to green flame retarded natural fiber reinforced PLA biocomposites.

Keywords: biopolymers; composites; flame retardance; natural fibres; thermal decomposition.

1 Introduction

Polylactic acid (PLA) is a biodegradable thermoplastic derived from renewable carbohydrate sources such as corn starch and sugarcane. Due to environmental considerations and ever growing demand for polymeric materials, it offers a promising alternative to plastics based on petrochemicals. PLA has found widespread applications in packaging, fibers and fabrics manufacturing (1, 2). However, extending the applicability of PLA to the transportation and electronics sectors while keeping its biodegradable and sustainable features intact poses significant challenges. First, the mechanical properties of PLA have to be improved using fiber reinforcement, more specifically natural fibers in order to keep the produced biocomposites environmentally sustainable. In addition, to effectively compete with technical polymers, efficient flame retarded composites of PLA must be introduced. To maintain the environmental advantages of using PLA and keeping the composites' mechanical properties optimal, it is, of course, desirable to employ the lowest possible amounts of ecologically acceptable inorganic additives used as flame retardants and adjuvants.

In the past decade several flame retarded PLA systems have been developed and discussed (3), including nanocomposites based on inorganic additives, such as metal oxides and hydroxides (4), nanomaterials (nanoclays (LS) and nanotubes) (5, 6) and phosphorous based intumescent flame retardants (7–13), as well as their combinations (14–17). Most of these flame retarded systems act predominantly in the condensed phase via the formation of an intumescent inorganic layer or char that reduces heat and fuel transfer.

Natural fiber reinforced polymer biocomposites have received increasing attention in the development of new materials with improved mechanical and fire retarded properties (6, 18–25). Among the different natural fibers, kenaf fibers are used in commercial applications because of their advantages like: availability, short time to harvest, and good mechanical properties (26). A few flame retarded kenaf composites have been proposed (22, 27, 28). In keeping with growing demand for green flame retarded polymeric materials, the application of halogen-free flame retardants such as $Mg(OH)_2$ (MH), ammonium polyphosphate (APP) or expandable graphite (EG) is preferred as they belong to the few commercial flame retardants recommended to be used with respect to environmental concerns (29). Yet, to maintain the mechanical properties of flame retarded polylactic acid (PLA) biocomposites, the flame retardant content must be limited. Therefore this work presents a systematic study of kenaf reinforced PLA

***Corresponding author: Bernhard Schartel,** Bundesanstalt für Materialforschung und –prüfung (BAM), Unter den Eichen 87, 12205 Berlin, Germany, e-mail: bernhard.schartel@bam.de
Fanni D. Sypaseuth, Emanuela Gallo and Serhat Çiftci: Bundesanstalt für Materialforschung und –prüfung (BAM), Unter den Eichen 87, 12205 Berlin, Germany

(K-PLA) using multicomponent flame retardant systems with a maximum amount of 20 wt% additives based on MH/nanofiller or EG/APP flame retardants.

MH is a well-known halogen-free flame retardant that is normally used in high amounts of up to 60 wt%, with consequent negative impacts on the material's mechanical properties (30–33). By contrast, much lower concentrations (3–10 wt%) of nanomaterials can be used to achieve improved fire behavior under forced-flaming conditions, because they influence the properties of the protecting residual layer formed upon combustion (34–37). Naturally, it would be of great interest to combine these additives in a synergistic system exploiting the advantages of each component, while keeping the overall additive concentrations as low as possible. The application of this intriguing concept to combine metal hydrates with nanoparticles has been discussed previously for flame retarded composites (38–41).

The other basic route towards multicomponent flame retarded K-PLA was to apply combinations of expandable graphite (EG) and ammonium polyphosphate (APP) flame retardants with or without LS nanofiller. EG has been shown to be an effective flame retardant acting in the condensed phase in fire retarded polypropylene flax composites (18). APP is commonly used in intumescent systems and decomposes to (poly)phosphoric acid and ammonia when exposed to high temperatures. The generated phosphoric acid accelerates residue formation by esterification of the polymer functional groups, while NH_3 acts as blowing agent (42–44). A recent study on the combination of EG and APP as flame retardants in PLA composites showed a synergistic effect at an EG:APP ratio of 3:1 with respect to the flammability properties of the materials determined by oxygen index (LOI) and UL 94 tests (45).

2 Experimental

2.1 Materials

Poly(lactic acid) (PLA) Ingeo 3051D (Nature Works, USA) was used as a matrix polymer. Kenaf fibers purchased from Kenaf Eco Fibers Italia S.p.A. (Guastalla, Italy) were received with a broad length distribution, including fibers over 10 mm in length, which were chopped to lengths between 0.2 and 2.3 mm for use as a bio-based filler component. The investigated flame retardants and adjuvants were: (MH) Magnifin H5A magnesium hydroxide (Albemarle, USA), Exolit AP462 ammonium polyphosphate (APP) (Clariant, Germany), Nord-Min 250 expandable graphite (EG) (Nordmann Rassmann, Germany), Cloisite 30B layered silicate (LS) (Southern Clay Products Inc., USA) and Sidistar (Si) spherical silicon dioxide (Elkem, Norway). Table 1 presents the names and compositions of the prepared materials.

Table 1: Names of the studied materials and their compositions in wt%.

Material	PLA	Kenaf	MH	EG	APP	Si	LS
PLA	100	–	–	–		–	–
K-PLA	80	20	–	–		–	–
K-PLA/15MH	65	20	15	–		–	–
K-PLA/5Si	75	20	–	–		5	–
K-PLA/5LS	75	20	–	–		–	5
K-PLA/15MH/5Si	60	20	15	–		5	–
K-PLA/15MH/5LS	60	20	15	–		–	5
K-PLA/15EG	65	20		15			
K-PLA/10EG/5APP	65	20	–	10	5	–	–
K-PLA/5EG/10APP	65	20		5	10		
K-PLA/15APP	65	20			15		
K-PLA/8EG/4APP/3LS	65	20		8	4		3
K-PLA/4EG/8APP/3LS	65	20		4	8		3

2.2 Sample preparation

All composites were compounded at the IPF Leibniz Institute of Polymer Research (Dresden, Germany). The materials were extruded on a ZSE 27 MAXX co-rotating twin screw extruder (Leistritz Extrusionstechnik GmbH, Nuremberg, Germany, $T_{max}=180°C$, drive: 300 rpm). PLA was dried overnight at $T=45°C$ before extrusion. The granulates obtained were dried for 2 days at $T=45°C$ and injection molded into cone calorimeter specimens on a 420 C 1000–250 Allrounder (Arburg, Loßburg, Germany, $T_{max}=180°C$, $T_{mold}=35°C$). Injection molding of LOI and UL 94 specimens was performed on a Ergotech 100/420-310 from Demag (Schwaig, Germany, $T_{max}=180°C$, $T_{mold}=40°C$).

2.3 Characterization

The thermal decomposition of the prepared composites was investigated under nitrogen atmosphere (30 mL min^{-1} flow) on a Netzsch-TG 209 ASC F1 Iris thermogravimetry (TG) device (Netzsch, Selb, Germany) at a heating rate of 10°C min^{-1} from $T=30°C$ to $T=900°C$ using a sample weight of $m=5$ and 10 mg for the EG/APP and for the MH/nanofiller systems, respectively. The evolved pyrolysis gases were transferred to a Tensor 27 Fourier-transformed infrared (FTIR) spectrometer from Bruker Optics (Ettlingen, Germany) via a heated transfer line.

LOI and UL 94 classification were determined in order to assess the materials' reaction to small flame. The LOI test was performed in accordance with ISO 4589 on a device from Fire Testing Technology (FTT, East Grindstead, UK) on samples ($127 \times 6.5 \times 3.2$) mm^3 in size. UL 94 classifications according to IEC 60695-11-10 were tested in a flame chamber by FTT (East Grindstead, UK) on samples $127 \times 12.7 \times 3.2$ mm^3 in size.

To evaluate the materials' burning behavior under forced-flaming conditions, the cone calorimeter was used in accordance with ISO 5660. The ($100 \times 100 \times 4$) mm^3 specimens were irradiated with a heat flux of 50 kW m^{-2} at a sample heater distance of $l = 35$ mm. K-PLA/MH/nanofiller composites were measured in aluminum foil trays, whereas K-PLA/EG/APP composites were measured using retainer frames. Depending on the sample holder used in cone calorimeter measurements, the results of the same material may vary somewhat.

The mechanical properties of the materials (dumbbell specimens Type 1A, dimensions according to DIN EN ISO 3167) were determined according to DIN EN ISO 527 using a Zwick Roell Z010 universal 10 kN testing system (Ulm, Germany) with a preload force of $F = 10$ N. The dumbbells were milled out of the injection molded plates for the cone calorimeter test. The speed for the E-modul was of 1 mm min^{-1} the testing speed was 50 mm min^{-1}. The strength at maximum elongation and the elongation to break was determined in a separate test with a testing speed of 5 mm min^{-1}. All samples were conditioned before testing for at least $t = 48$ h at $50 \pm 5\%$ relative humidity and a temperature of $T = 23 \pm 2$°C. Five specimens of each material were tested and the mean values of the parameters were used.

3 Results and discussion

3.1 K-PLA/MH composites – mechanical properties

Fire retarded PLA materials should exhibit appropriate mechanical properties to be considered as useful technical polymers. Therefore fiber reinforced PLA materials were prepared using short kenaf natural fibers up to 2 mm long. Table 2 summarizes the mechanical properties of K-PLA, K-PLA/15MH, K-PLA/5Si, K-PLA/5LS, K-PLA/15MH/5Si and K-PLA/15MH/5LS formulations. K-PLA showed a tensile strength of about 59 MPa, 3.6% elongation at break and an E modulus of 3650 MPa. The kenaf fibers used were neither optimized with respect to mechanical reinforcement nor were any compatibilizers added, so that the mechanical properties achieved (E modulus = 4780 MPa) are superior to those of PLA, but the effect may be somewhat limited. Particular the elongation to break was halved. However, the idea was to investigate realistic composition of the composites and monitor the impact of flame retardants. Adding MH to K-PLA resulted in the formation of a stiffer composite (K-PLA/15MH), yielding tensile strength values 30% lower, and elongation at break values 50% lower than for K-PLA, whereas the E modulus increased by 25%. Due to this change in mechanical properties, the lowest possible amount of MH flame retardant should be used in biocomposite formulations, as is proposed here. Actually both limiting the content and taking additional actions to improve mechanical compatibility seem advisable. Spherical silicon dioxide (Si) and layered silicate (LS) were applied in K-PLA also to investigate their effects on the mechanical properties. K-PLA containing 5% of Si, K-PLA/5Si, show mechanical performance very similar to K-PLA, whereas LS in K-PLA/5LS increased E modulus and decreased the elongation to break. Applying the combinations with MH in K-PLA/15MH/5Si and K-PLA/15MH/5LS, respectively, yielded the highest E moduli of all investigated materials in this study up to two times the E modulus of PLA. The mechanical reinforcement achieved by the flame retardants outperforms the effect of the kenaf fibers. However, K-PLA/15MH/5Si and K-PLA/15MH/5LS showed elongations to break even lower than K-PLA/15MH underlining the need to optimize such systems with compatibilizer and limiting the amount of fillers.

Table 2: Mechanical properties of PLA/kenaf bio-composites containing MH flame retardant and silicon based nanofillers.

Material	E modulus (MPa)	Tensile strength at max (MPa)	Elongation at break (%)
PLA	3650 ± 110	58.8 ± 0.9	3.60 ± 0.57
K-PLA	4780 ± 40	52.2 ± 0.5	1.35 ± 0.02
K-PLA/15MH	5870 ± 80	37.6 ± 0.8	0.66 ± 0.02
K-PLA/5Si	4560 ± 100	52.1 ± 0.9	1.60 ± 0.06
K-PLA/5LS	5520 ± 170	48.2 ± 1.8	1.01 ± 0.04
K-PLA/15MH/5Si	6200 ± 90	33.7 ± 0.4	0.56 ± 0.01
K-PLA/15MH/5LS	6740 ± 110	30.8 ± 0.7	0.46 ± 0.02

3.2 K-PLA/MH composites – pyrolysis and thermal decomposition

Figure 1 shows the mass loss and mass loss rate curves of PLA, K-PLA, K-PLA/15MH, K-PLA/5Si, K-PLA/5LS, K-PLA/15MH/5Si and K-PLA/15MH/5LS obtained for

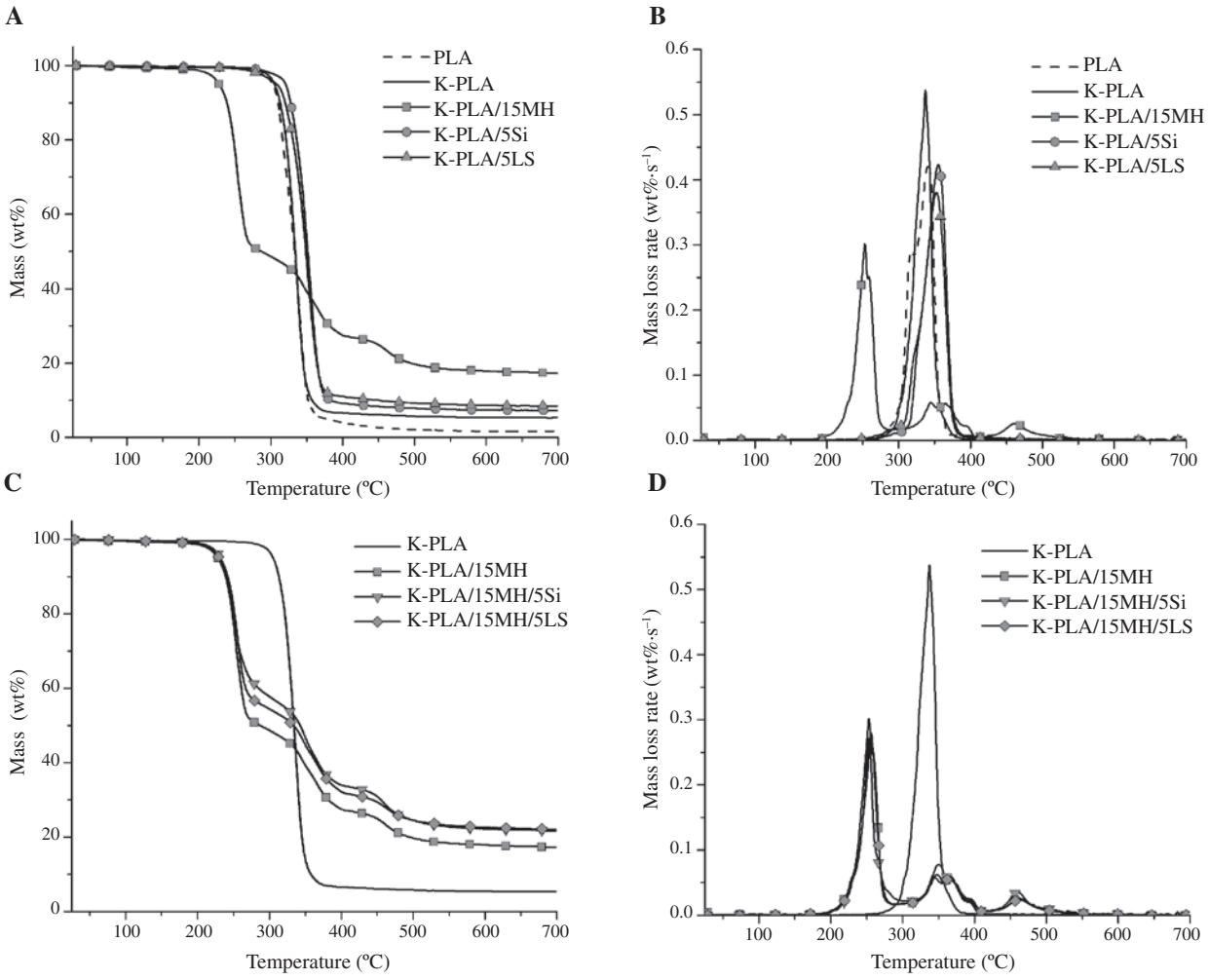

Figure 1: (A) Mass loss (ML) and (B) mass loss rate (MLR) curves of PLA, K-PLA and K-PLA composites with MH, Si and LS as single fillers; (C) ML and (D) MLR of combinations MH/Si and MH/LS.

TG-FTIR measurements. Under pyrolysis conditions, PLA and K-PLA both started to decompose at about 290°C and showed similar decomposition behavior, except that PLA underwent an additional slight mass loss directly after the first decomposition step. Between 300 and 400°C, the mass losses were 96 and 93 wt% for PLA and K-PLA, respectively (see Table 3). K-PLA yielded a higher amount of residue, 5.3 wt% compared to 1.7 wt%

Table 3: Thermogravimetry results (N_2, error ±1 K, ±1 wt%) of PLA, K-PLA and K-PLA composites with LS, Si, MH and combinations; residue value was taken at 700°C.

Material	200°C–300°C			300°C–400°C		400°C–550°C		Residue wt%
	$T_{2\%}$ (°C)	T_{max} (°C)	ML (wt.%)	T_{max} (°C)	ML (wt.%)	T_{max} (°C)	ML (wt.%)	
PLA	289			341	96			1.7
K-PLA	292			337	93			5.3
K-PLA/5Si	300			357	92			7.6
K-PLA/5LS	282			354	90			8.4
K-PLA/15MH	211	253	51	344	22	461	9	17.6
K-PLA/15MH/5Si	218	254	43	351	23	461	11	22.2
K-PLA/15MH/5LS	213	261	45	347	23	460	8	22.3

for PLA. K-PLA/5Si and K-PLA/5LS also decomposed in a single step between 300 and 400°C, with a considerable mass loss of 92 and 90 wt%, respectively. K-PLA/5LS started to decompose at a lower temperature of $T = 282$°C due to the loss of the organic modifier in the layered silicate (for single component LS $T_{onset} = 240$°C), whereas the temperature of the maximum mass loss rate shifted to $T_{max} = 354$°C, 17°C higher than that of K-PLA. A similar effect was observed in the presence of Si filler, except in this case the whole TG curve shifted to higher temperatures due to the high thermal stability of Si. The reduced mass loss rate of K-PLA with Si or LS compared to K-PLA confirms the effect of the hindered release of volatiles during pyrolysis in the presence of these fillers. For both K-PLA/5Si and K-PLA/5LS the amounts of residue increased to about 8 wt% at $T = 700$°C, compared to 5 wt% in the case of K-PLA.

In the case of materials containing MH (K-PLA/15MH, K-PLA/15MH/5Si and K-PLA/15MH/5LS), the pyrolysis behavior changed completely, showing three main steps between $T = 200$–300, 300–400 and 400–550°C. MH thermally destabilized the materials to a great extent, resulting in a decrease in initial decomposition temperature ($T_{2\%}$) of about 70–80°C compared to that of K-PLA. Moreover, mass losses of 51 wt% for K-PLA/15MH and about 40 wt% for K-PLA/15MH/5Si and K-PLA/15MH/5LS were observed, attributed to PLA and kenaf decomposition. As the mass loss in this first decomposition step is lower than expected from the pyrolysis behavior of K-PLA (ML = 93 wt%, so for K-PLA/15MH/5nanofiller the ML expected mass loss due to K-PLA decomposition is 0.93·80 wt% = 74.4 wt%), additional charring during pyrolysis is proposed for the materials containing MH. The second decomposition step of K-PLA/MH materials is an overlap between kenaf and MH decomposition, showing a mass loss of about 20% and the highest H_2O release rate. Above temperatures of T_{max} in the second decomposition step, the mass of the residue is higher than expected from the TG curves of single components, indicating increased charring of the K-PLA/MH materials, which produced stable residues up to 450°C. The third step was attributed to further decomposition of the K-PLA/MH residue, with mass losses between 8 and 11 wt% leaving a final residual mass still higher than expected for the superposition of the single components, which supports the positive effect of the MH additive on char formation and stability. Si and LS are inert fillers and therefore had no influence on the general decomposition behavior of the composites. They affected only the mass loss in the first decomposition step and the final residual mass according to their amounts in the composites.

3.3 K-PLA/MH composites – reaction to small flame

PLA has a LOI of 23 vol% and is V-2 classified in UL 94 tests (Table 4). In the UL 94 test the fire extinguished upon dripping, indicating removal of fuel and heat from the pyrolysis zone. The presence of kenaf fiber prevented dripping of the composites, resulting in no extinguishment in UL 94 tests, so that all K-PLA materials received HB classification. Similarly, for K-PLA the LOI value decreased to 17 vol%, due to retention of the material in the pyrolysis zone fueling the flame (46–48). Addition of 15 wt% MH increased the LOI by 3 vol% due to dilution and cooling effects as well as additional residue formation. The addition of LS or Si in the absence of MH enhanced the formation of a protective barrier and increased the LOI by 3–5 vol% compared to K-PLA. The LOI in the presence of both MH and the nanofillers Si or LS showed a close to negligible effect compared to the LOI of K-PLA/15MH. The LOI achieved seems disappointing, but this is misleading, as similar systems have previously been reported to achieve UL 94 V-1 classification with LOI of 23 vol. % (49).

3.4 K-PLA/MH composites – forced-flaming burning behavior

Under forced-flaming conditions, PLA presented the burning behavior of a typical non-charring material, with the HRR increasing steadily after ignition until the PHRR of 662 kW m^{-2} was reached, followed by a decrease in HRR as all material was consumed during pyrolysis (Figure 2A, B) (50). Similarly, for each material studied an increase in HRR was observed directly after ignition. Interestingly, in the case of K-PLA the time to ignition decreased to $t_{ig} = 22$ s from $t_{ig} = 38$ s for PLA, probably due to an increase in viscosity and no heat convection in the melt (Table 5) (51).

K-PLA/15MH containing 15% of MH ignited faster than all other materials, with the lowest time to ignition

Table 4: Reaction to small flame tests: oxygen index (LOI) and UL 94 of PLA and K-PLA with MH and adjuvants Si/LS.

Material	LOI/vol.-%	UL 94
PLA	23	V-2
K-PLA	17	HB
K-PLA/15MH	20	HB
K-PLA/5Si	20	HB
K-PLA/5LS	22	HB
K-PLA/15MH/5Si	21	HB
K-PLA/15MH/5LS	22	HB

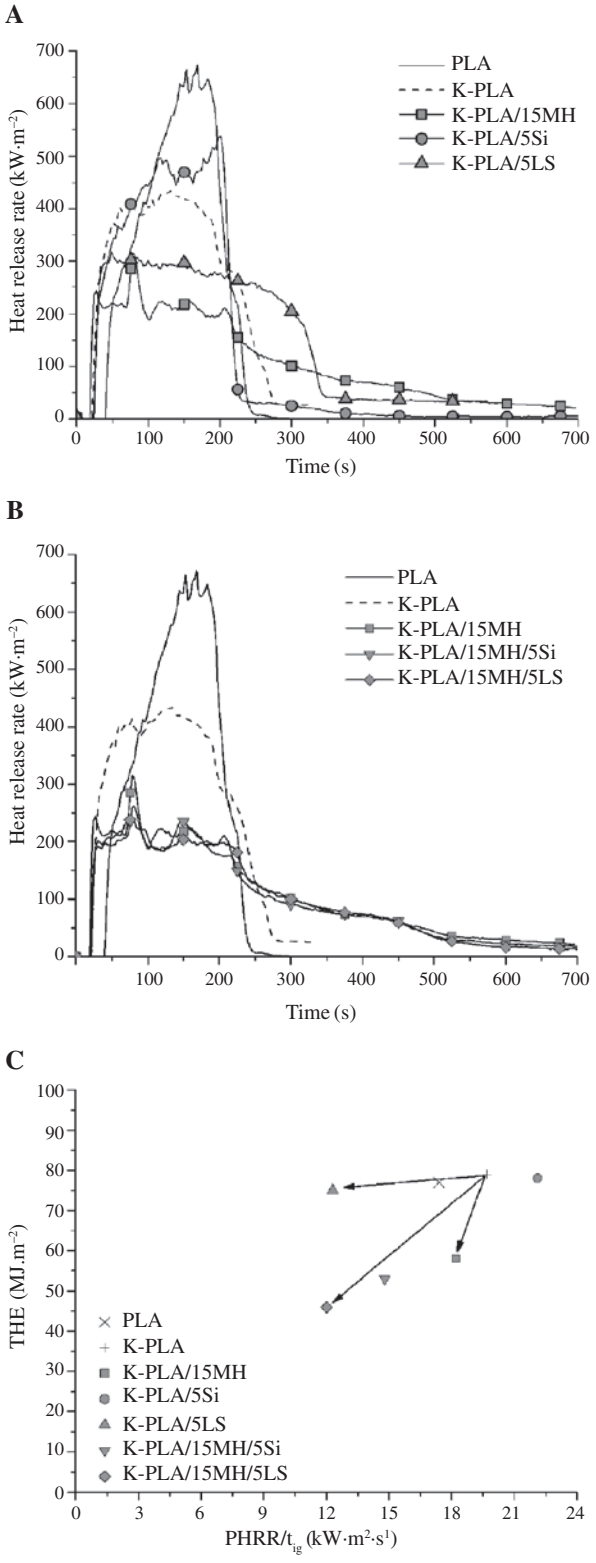

Figure 2: (A) Heat release rate (HRR) curves of PLA, K-PLA and K-PLA composites with MH, Si and LS as single fillers; (B) HRR of combinations MH/Si and MH/LS; (C) Petrella plot assessing the fire risk of K-PLA composites with MH, Si, LS and their combinations by plotting fire load/total heat evolved (THE) vs. flame spread indication parameter PHRR/t_{ig}.

of t_{ig} = 17 s, even though MH typically cools and dilutes the flame and pyrolysis zones, decreasing the critical oxygen-fuel ratio. These results are in agreement with findings from the TG measurements, namely that for K-PLA/15MH enhanced pyrolysis of PLA and kenaf was observed at temperatures between T = 200 and 300°C (Figure 1). A PHRR of 309 kW m^{-2} was observed for K-PLA/15MH upon cracking of the initial protecting layer and the sudden release of flammable volatiles. The cracking of the protective layer is clearly visible on the fire residue of K-PLA/15MH depicted in Figure 3B. Subsequently, HRR decreased again as further residue gradually formed. The THE of K-PLA/15MH decreased to THE = 58 mJ m^{-2} from THE = 79 mJ m^{-2} for K-PLA (Table 5). In the presence of nanofillers without MH the time to ignition increased to t_{ig} = 24 s and the THE values were similar to that of K-PLA, about 30% higher than for materials containing MH. In the case of K-PLA/5Si, a slightly higher PHRR was recorded, which indicates a lower quality protective layer, whereas K-PLA/5LS exhibited an HRR that decreased steadily after initial growth, suggesting a stabler closed residue (Figure 2A). The better quality of residue for K-PLA/5LS compared to K-PLA/5Si can also be deduced from the fire residues shown in Figure 3C and D, respectively. When both MH and nanofiller were added to the composites, the PHRR values were lower, with a sharp peak that implied the formation of an initial unstable protective layer, after which the HRR curve gradually levelled off. In both cases the THE decreased to 30–40% below the value obtained with K-PLA (Figure 2B). PLA and K-PLA had a very similar effective heat of combustion, with values of THE/ML = 1.7 and 1.6 mJ m^{-2} g^{-1}, respectively. The THE/ML value was not influenced by the addition of the nanofillers Si or LS. When MH was present in the biocomposites, the THE/ML values decreased to 1.5 mJ m^{-2} g^{-1} for K-PLA/15MH and K-PLA/15MH/5LS, and to 1.4 mJ m^{-2} g^{-1} for K-PLA/15MH/5Si. The slight decrease in effective heat of combustion in the presence of MH indicates a dilution effect of the fuel under forced-flaming conditions, due to the release of water from the decomposition of MH.

Figure 2C shows the overall flame retardancy effect of MH, Si and LS additives and their combinations. K-PLA had a fire load similar to PLA, being more prone to quickly developing fire, as shown by the increased PHRR/t_{ig} value (Figure 2C and Table 5). Upon addition of Si or LS to K-PLA, the THE value of K-PLA was retained, but a significant difference between the flame spread characteristics of these two composites was observed. K-PLA/5Si, having the same t_{ig} value but a much higher PHRR than K-PLA/5LS, is more likely to promote a quickly developing fire (Table 5). In the presence of MH the fire load decreased significantly and the fire spread characteristics

Table 5: Fire properties (cone calorimeter, 50 kW m^{-2} irradiation).

Material	t_{ig} (s)	PHRR (kW m^{-2})	THE (mJ m^{-2})	Residue (wt.%)	THE/ML (mJ m^{-2} g^{-1})	PHRR/t_{ig} (kW m^{-2} s^{-1})	MARHE (kW m^{-2})
PLA	38	662±26	77±3	8	1.7	17.4	372±11
K-PLA	22	433±17	79±3	6	1.6	19.7	334±8
K-PLA/15MH	17	309±12	58±2	28	1.5	18.2	192±6
K-PLA/5Si	24	530±21	78±3	10	1.7	22.1	384±10
K-PLA/5LS	24	295±12	75±3	12	1.7	12.3	239±20
K-PLA/15MH/5Si	19	281±11	53±2	33	1.4	14.8	186±6
K-PLA/15MH/5LS	21	251±10	46±2	44	1.5	12.0	186±6

t_{ig}, time to ignition; PHRR, peak heat release rate; THE, total heat evolved; ML, mass loss; uncertainty for t_{ig}: ±2 s; for residue: ±1 wt%; for THE/ML: ±0.1 mJ m^{-2} g^{-1}.

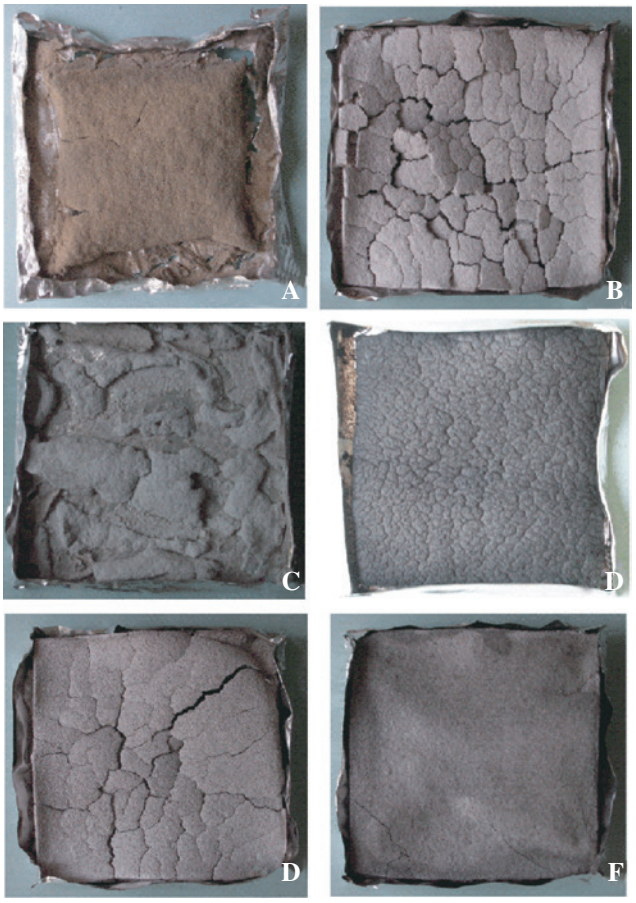

Figure 3: Cone calorimeter residues of (A) K-PLA, (B) K-PLA/15MH, (C) K-PLA/5Si, (D) K-PLA/5LS, (E) K-PLA/15MH/5Si and (F) K-PLA/15MH/5LS.

also improved compared to those of K-PLA. Addition of nanofillers to K-PLA/15MH improved the THE and PHRR/t_{ig} values for both K-PLA/15MH/5Si and K-PLA/15MH/5LS materials, with K-PLA/15MH/5LS proving to be the superior composite and best material in terms of overall fire behavior. MARHE analysis revealed the same overall trend for the flame retardancy features of the various materials; however, the fire spread characteristics were much more similar for K-PLA/15MH, K-PLA/15MH/5Si and K-PLA/15MH/5LS materials, while K-PLA showed better fire spread characteristics than PLA (Table 5).

3.5 K-PLA intumescent composites – mechanical properties

As shown in Table 6, the tensile strength of biocomposites in the presence of EG decreased by 50% and in the presences of APP by 19% compared to that of K-PLA. The elongation in break was reduced in an analogous manner. The tensile strength at maximum of the flame retardant mixtures K-PLA/10EG/5APP, K-PLA/5EG/10APP, K-PLA/8EG/4APP/3LS, and K-PLA/4EG/8APP/3LS was in between the one for K-PLA/15EG and K-PLA/15APP. Surprisingly, K-PLA/10EG/5APP, K-PLA/5EG/10APP, K-PLA/8EG/4APP/3LS, and K-PLA/4EG/8APP/3LS show larger elongations to break, particular the systems for which EG/APP is replaced by LS show elongations to break only 14% less than K-PLA. The E moduli of the flame retarded systems increased by around 15% compared to K-PLA and up to 52% compared to PLA. The EG/APP systems yielded mechanical reinforcement. The reduction in elongation to break by the flame retardants was less pronounced than it occurred for the MH systems.

3.6 K-PLA intumescent composites – pyrolysis and thermal decomposition

In thermogravimetric analysis, all materials decomposed between 250 and 400°C, and the flame retarded systems containing EG, APP or their combinations decomposed in two steps independent of the EG:APP ratio (Figure 4). Addition of EG or APP decreased the initial decomposition temperature ($T_{2\%}$) significantly, due to decomposition of

Table 6: Mechanical properties of PLA/kenaf bio-composites containing expandable graphite (EG) and/or ammonium polyphosphate (APP) flame retardants and layered silicate (LS) nanofiller.

Material	E modulus (MPa)	Tensile strength at max (MPa)	Elongation at break (%)
PLA	3650 ± 110	58.8 ± 0.9	3.60 ± 0.57
K-PLA	4780 ± 40	52.2 ± 0.5	1.35 ± 0.02
K-PLA/15EG	5310 ± 30	26.5 ± 2.2	0.62 ± 0.06
K-PLA/10EG/5APP	5540 ± 80	33.3 ± 0.2	1.01 ± 0.07
K-PLA/5EG/10APP	5560 ± 80	35.9 ± 0.4	1.14 ± 0.02
K-PLA/15APP	5510 ± 110	42.4 ± 1.9	0.99 ± 0.03
K-PLA/8EG/4APP/3LS	5500 ± 80	31.9 ± 0.2	1.15 ± 0.05
K-PLA/4EG/8APP/3LS	5240 ± 60	30.9 ± 1.1	1.17 ± 0.15

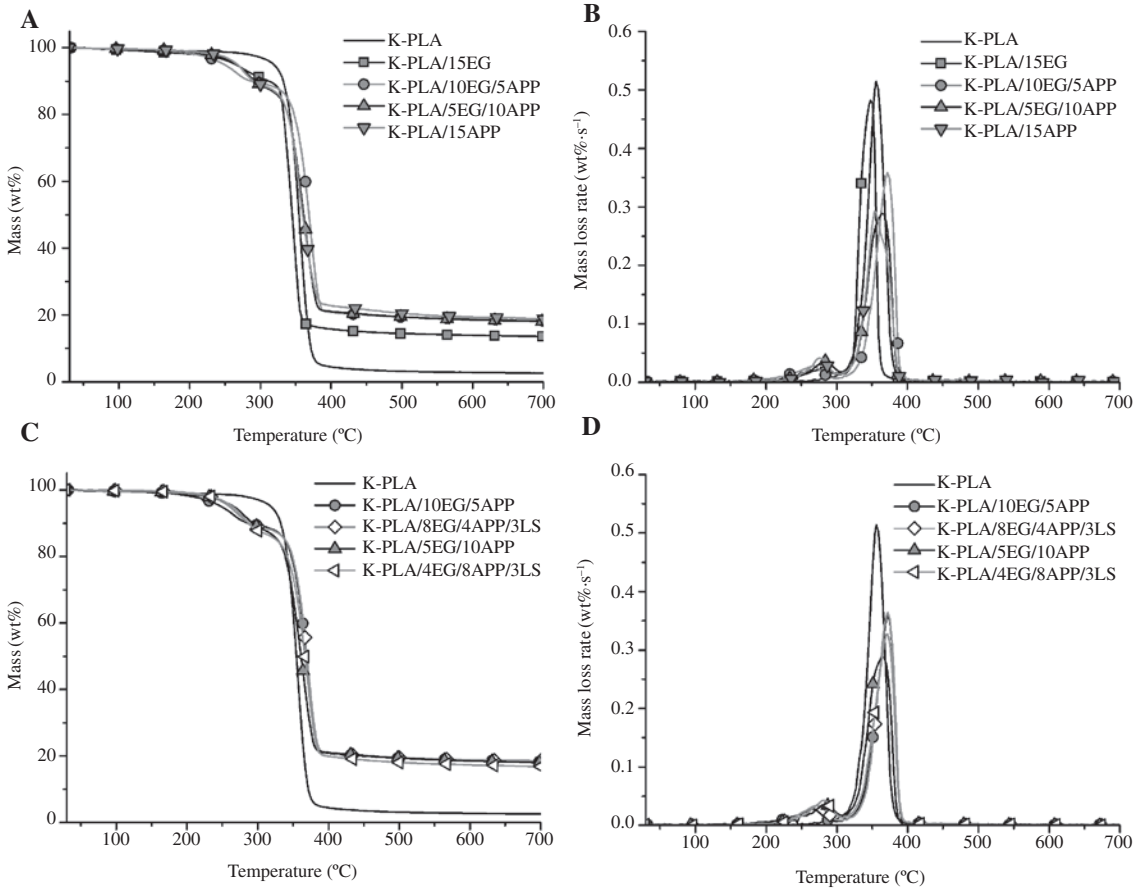

Figure 4: (A) Mass loss (ML) and (B) mass loss rate (MLR) curves of K-PLA composites with intumescent systems with varying EG:APP ratios; (C) ML and (D) MLR of intumescent systems of 2:1 and 1:2 EG:APP ratio with and without LS nanofillers.

the flame retardants (Table 7). A higher EG ratio resulted in lower $T_{2\%}$, indicating less thermal stability of the biocomposites in the presence of EG, which decomposes to CO_2, SO_2 and H_2O at temperatures above 200°C (52). In the first decomposition step the mass loss observed when APP and EG were both present in the material was higher than for K-PLA/15EG due to the release of H_3PO_4 from APP, which accelerates kenaf decomposition via phosphorylation of the hydroxyl groups in the cellulosic structure of kenaf (53). The second decomposition step is related to PLA and kenaf decompositions, and occurred for all materials at around 350°C. In the case of K-PLA/15APP, the mass loss in the second step decreased to 70.7%, whereas in the presence of 15 wt% EG the mass loss was 77.1%. The positive effect of APP on the mass loss in the second decomposition step was observed even at the lowest amount of APP

Table 7: Thermogravimetry results (N_2, error ±1 K, ±1 wt%) of K-PLA and K-PLA composites with intumescent EG/APP systems of varying EG:APP ratios and their combinations with LS; residue values were taken at 760°C.

Material	200°C–300°C			300°C–400°C		Residue (wt%)
	$T_{2\%}$ (°C)	T_{max} (°C)	ML (wt.%)	T_{max} °C	ML (wt.%)	
K-PLA	282			356	93	5.3
K-PLA/15EG	211	278	7.6	351	77.1	13.3
K-PLA/10EG/5APP	206	266	8.5	371	71.8	18.9
K-PLA/5EG/10APP	230	284	9.6	364	70.7	17.7
K-PLA/15APP	240	277	9.1	354	70.7	18.1
K-PLA/8EG/4APP/3LS	238	270	9.0	372	70.8	18.2
K-PLA/4EG/8APP/3LS	236	281	10.8	371	70.3	16.9

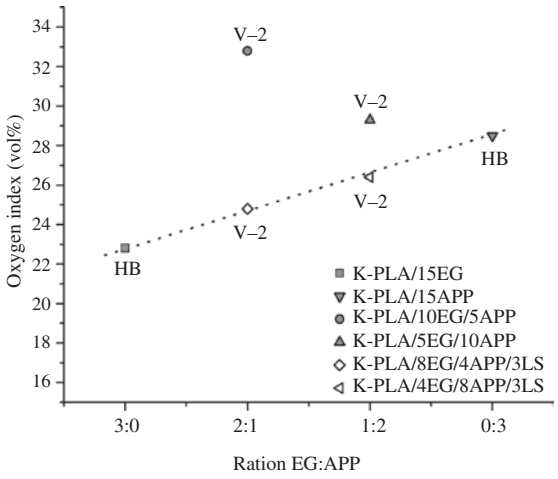

Figure 5: Oxygen index and UL 94 classification as a function of the EG:APP ratio in K-PLA; without and with LS nanofillers.

(K-PLA/10EG/5APP), yielding a mass loss of ML = 71.8%. When both EG and APP additives were present in the composites, the second decomposition step occurred at higher temperatures. Using 3 wt% layered silicate nanofiller while keeping the total additive amount at 15 wt% and the EG:APP ratio at 2:1 or 1:2 resulted in increased initial decomposition temperatures of $T_{2\%} = 238$°C for K-PLA/8EG/4APP/3LS and $T_{2\%} = 236$°C for K-PLA/4EG/8APP/3LS and slightly higher mass loss values in the first decomposition step, while the ML values remained in the second step. Due to the synergistic effect, the amount of residue was higher when both EG and APP were added to the composite and it was the highest in the case of an EG:APP ratio of 2:1 in the presence or the absence of layered silicate.

3.7 K-PLA intumescent composites – reaction to small flame

Addition of 15 wt% EG to K-PLA increased the LOI from 17 vol% to 22.3 vol%. When a combination of the two fire retardants was used in the biocomposite, the LOI value increased to 29.3 and 32.8 vol% for an EG:APP ratio of 1:2 and 2:1, respectively. Supporting the findings from TG measurements, the LOI values also show that the synergistic effect between EG and APP is more pronounced in the specific ratio of 2:1. In the presence of LS nanofiller the LOI values dropped significantly, while the synergistic effect between EG and APP diminished (Figure 5). The negative effect of nanocomposites on LOI has been reported before (54). Nanocomposites are more prone to ignition at lower oxygen levels, because nanofillers increase melt viscosity, resulting in hindered intumescence, less material dripping and therefore more available fuel in the pyrolysis zone. When single component fire retardants were used, e.g. in K-PLA/15EG and K-PLA/15APP, the materials failed the vertical UL 94 test and were classified as HB. All samples containing a combination of EG and APP as fire retardants achieved V-2 classification both in the presence and the absence of LS nanofiller. While V-2 classification is obviously an improvement over HB, for technical purposes V-0 classification is required, thus further optimization of the fire retardant systems is needed.

3.8 K-PLA intumescent composites – forced-flaming burning behavior

Composites containing the single component flame retardants EG or APP (K-PLA/15EG and K-PLA/15APP, respectively) showed the behavior of charring materials according to their HRR curve (Figure 6), with about 20 wt% residue remaining in both cases (Table 8, Figure 7, see also the fire residues in Figure 8B and E) (50). The HRR decreased after an initial increase due to reduced heat and mass transfer caused by charring (Figure 6A). In the case of K-PLA/15EG, the initial char layer created by the expandable graphite cracked as trapped combustible volatiles were released, causing fluctuations in the recorded HRR curve. K-PLA/15APP yielded a stable HRR curve, and for both flame retarded systems the PHRR decreased significantly compared to K-PLA, by 24 and 28% for K-PLA/15EG and K-PLA/15APP, respectively (Figure 7A).

When combinations of the flame retardants EG and APP were used, in both cases an initial growth in the HRR was observed, and there was also a second local maximum after the PHRR due to the sudden release of

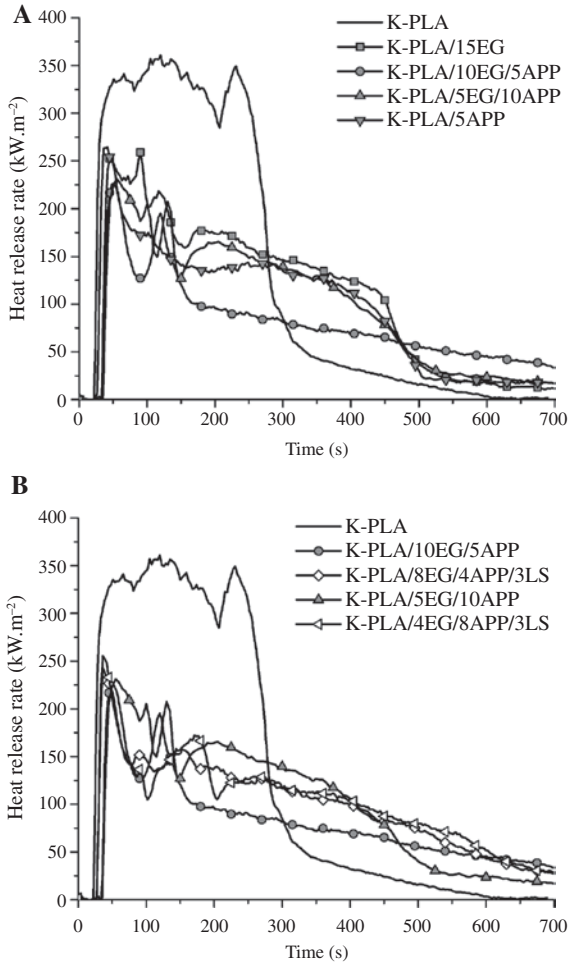

Figure 6: (A) Heat release rate (HRR) curves of K-PLA composites with intumescent systems with varying EG:APP ratios; (B) HRR of intumescent systems with EG:APP ratios of 2:1 and 1:2, with and without nanofillers LS.

pyrolysis gases upon cracking of the protective layer, as in the case of K-PLA/15EG (see fire residues in Figure 8C and D). K-PLA/5EG/10APP showed the HRR curve of a charring material, whereas the HRR curve of K-PLA/10EG/5APP levelled off gradually after the second local maximum of HRR (Figure 6A). The combinations of flame retardants in both 2:1 and 1:2 ratios resulted in a higher decrease in PHRR compared to K-PLA (37 and 33% for K-PLA/10EG/5APP and K-PLA/5EG/15APP, respectively) than when either EG or APP was used as single component. The largest decrease of 37% was observed at an EG:APP ratio of 2:1, for K-PLA/10EG/5APP (Figure 7A). Similarly, the most significant decrease of 39% in THE compared to K-PLA was also observed for K-PLA/10EG/5APP, with a value of THE = 63 mJ m^{-2}. The increase in residue was also highest for K-PLA/10EG/5APP, with 32 wt%. The THE/ML value of 1.7 kW m^{-2} g^{-1} for K-PLA did not decrease in the presence of 15 wt% EG for K-PLA/15EG, but the values improved slightly for composites containing APP or a combination of EG and APP to 1.5 kW m^{-2} g^{-1} due to dilution of the fuel by the release of H_2O from APP decomposition (Table 8). In summary, Figures 7A, B and C show the significant synergistic effect between the two flame retardants at a ratio of EG:APP = 2:1 on the PHRR, THE and the amount of residual mass in K-PLA/10EG/5APP biocomposite.

Addition of layered silicate to the composite delayed the cracking of the char in the case of K-PLA/4EG/8APP/3LS with an EG:APP ratio of 1:2, by increasing the melt viscosity and char strength (Figure 6B). The mass loss rate of K-PLA/4EG/8APP/3LS under forced-flaming conditions was also lower than in the absence of LS, because the char hampered the release of the NH_3 formed during the APP decomposition. Similarly, for this material the second local maximum on the HRR curve was absent, because a stronger char formed, which underwent less cracking and released lower amounts of volatile pyrolysis products. When the ratio of EG:APP was 2:1 in K-PLA/8EG/4APP/3LS, a local maximum in the HRR curve was also not observed. The THE values of both K-PLA/8EG/4APP/3LS and K-PLA/4EG/8APP/3LS were reduced by 25% compared to K-PLA (Figure 7B). The PHRR

Table 8: Fire properties obtained using a cone calorimeter with 50 kW m^{-2} irradiation.

Material	t_{ig} (s)	PHRR (kW m^{-2})	THE (mJ m^{-2})	Residue (wt.%)	THE/ML (mJ m^{-2} g^{-1})	PHRR/t_{ig} (kW m^{-2} s^{-1})	MARHE (kW m^{-2})
K-PLA	27	355	88	2	1.7	13.1	290 ± 5
K-PLA/15EG	29	270	73	19	1.7	9.3	175 ± 9
K-PLA/10EG/5APP	39	222	53	34	1.5	5.7	118 ± 5
K-PLA/5EG/10APP	35	237	67	18	1.5	6.8	150 ± 5
K-PLA/15APP	31	254	63	22	1.5	8.2	142 ± 4
K-PLA/8EG/4APP/3LS	30	248	66	25	1.6	8.3	139 ± 8
K-PLA/4EG/8APP/3LS	27	247	66	21	1.5	9.1	134 ± 5

t_{ig}, time to ignition; PHRR, peak heat release rate; THE, total heat evolved; ML, mass loss; error of measurement for t_{ig}: ±2 s; for residue: ±1 wt.%; for THE/ML: ±0.1 mJ m^{-2} g^{-1}.

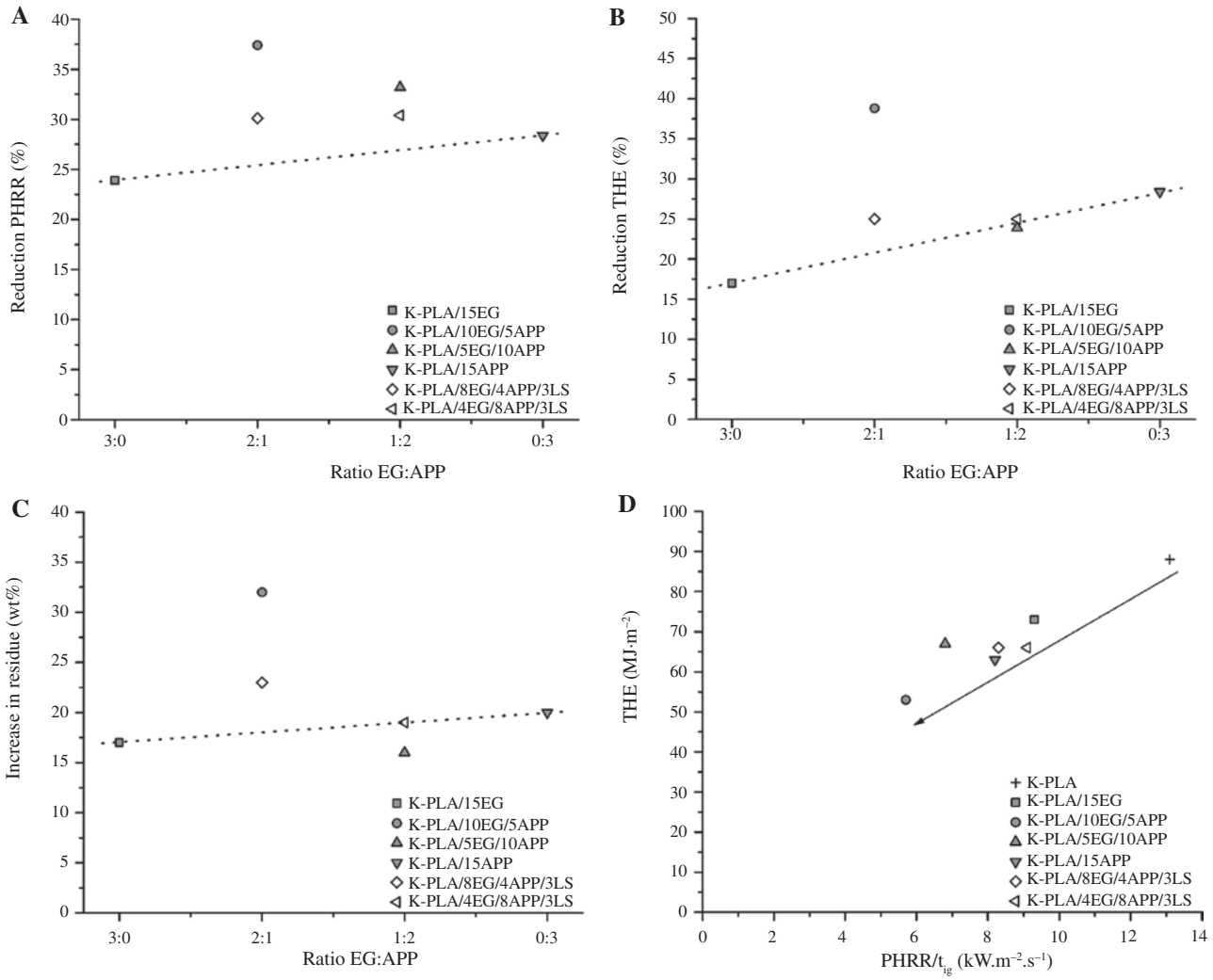

Figure 7: (A) Reduction of peak HRR, (B) reduction of THE and (C) increase in fire residue as a function of the EG:APP ratio in comparison to K-PLA, without and with LS; (D) Petrella plot assessing the fire risk of intumescent flame retarded K-PLA composites by plotting fire load/total heat evolved (THE) vs. flame spread indication parameter PHRR/t_{ig}.

values for K-PLA/8EG/4APP/3LS and K-PLA/4EG/8APP/3LS were about 30% lower than that of K-PLA (Figure 7A). Addition of LS did not influence the THE/ML values compared to the other flame retarded composites containing combinations of EG and APP.

Figure 7D summarizes the fire load of the different materials as well as their fire spread characteristics. According to the PHRR/t_{ig} analysis, materials containing a mixture of flame retardants are less prone to quickly developing fire than materials with a single component fire retardant due to an increase in time to ignition as well as a decrease in PHRR values. However, the total heat evolved by K-PLA/5EG/10APP was similar to that of the other flame retarded systems and only K-PLA/10EG/5APP showed a lower fire load. Considering the MARHE values, which also describe the fire spread characteristics, K-PLA/15EG showed the worst properties (MARHE = 175 ± 9 kW m^{-2}) and would support a quickly developing fire, whereas K-PLA/10EG/5APP gave the lowest MARHE value of 118 ± 5 kW m^{-2}. All the other materials showed very similar MARHE values between 134 and 150 kW m^{-2}.

4 Conclusion

This paper discusses the basic routes for using reasonable amounts of flame retardants and nanofillers in K-PLA biocomposites for technical applications. The results of this feasibility study show improved fire properties of the flame retarded biocomposites under forced-flaming conditions with significant reductions in THE, PHRR and MARHE values. Both approaches of using MH with nanofillers

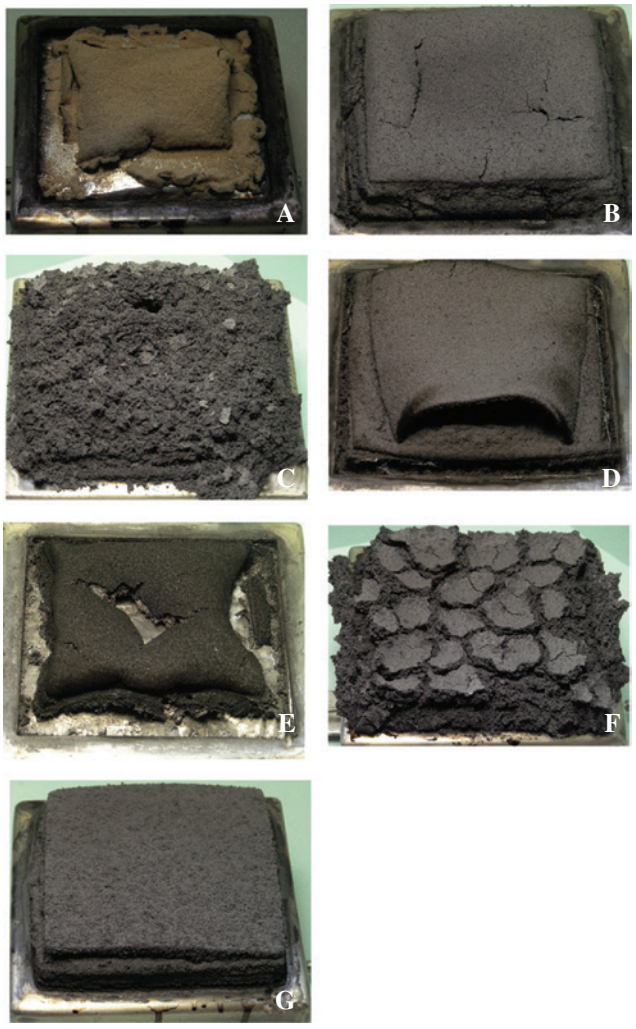

Figure 8: Cone calorimeter residues of (A) K-PLA, (B) K-PLA/15EG, (C) K-PLA/10EG/5APP, (D) K-PLA/5EG/10APP, (E) K-PLA/15APP, (F) K-PLA/8EG/4APP/3LS and (G) K-PLA/4EG/8APP/3LS.

and EG/APP mixtures affected fire behavior by dilution of the flame upon FR decomposition and the formation of a protective layer that hinders fuel and heat transfer. The best results were obtained when using multicomponent systems such as K-PLA/15MH/5LS and K-PLA/10EG/5APP rather than single component flame retardants. In the case of EG/APP combinations, synergistic effects were observed at a ratio of 2:1 in terms of LOI, THE, PHRR values, the amount of residue as well as fire spread characteristics. In both systems the amount of additives could be kept at as low as 15–20 wt% while achieving efficient flame retardancy. Although the mechanical properties of the biocomposites were not optimized and the UL 94 tests showed V-2 classification at best, the principle routes towards completely green flame retarded PLA biocomposites were successfully presented.

Acknowledgments: The authors thank E. Lorenz and D. Schulze for their contribution to the mechanical tests of the composites and B. Dittrich for her input in the preparation of the manuscript.

References

1. Jamshidian M, Tehrany EA, Imran M, Jacquot M, Desobry S. Poly-lactic acid: production, applications, nanocomposites, and release studies. Compr Rev Food Sci Food Saf. 2010;9:552–71.
2. Garlotta D. A literature review of poly(Lactic acid). J Polym Environ. 2001;9:63–84.
3. Bourbigot S, Fontaine G, Gallos A, Bellayer S. Reactive extrusion of PLA and of PLA/carbon nanotubes nanocomposite: processing, characterization and flame retardancy. Polym Adv Technol. 2011;22:30–7.
4. Yanagisawa T, Kiuchi Y, Iji M. Enhanced flame retardancy of polylactic acid with aluminum tri-hydroxide and phenolic resins. Kobunshi Ronbunshu. 2009;66:49–54.
5. González A, Dasari A, Herrero B, Plancher E, Santarén J, Esteban A, Lim SH. Fire retardancy behavior of PLA based nanocomposites. Polym Degrad Stab. 2012;97:248–56.
6. Hapuarachchi TD, Peijs T. Multiwalled carbon nanotubes and sepiolite nanoclays as flame retardants for polylactide and its natural fibre reinforced composites. Compos Part A. 2010;41:954–63.
7. Xi W, Qian LJ, Qiu Y, Chen YJ. Flame-retardant behavior of bi-group molecule derived from phosphaphenanthrene and triazine groups on polylactic acid. Polym Adv Technol. 2016;27:781–8.
8. Tang G, Huang X, Ding H, Wang X, Jiang S, Zhou K, Wang B, Yang W, Hu Y. Combustion properties and thermal degradation behaviors of biobased polylactide composites filled with calcium hypophosphite. RSC Adv. 2014;4:8985.
9. Fox DM, Lee J, Citro CJ, Novy M. Flame retarded poly(lactic acid) using POSS-modified cellulose. 1. Thermal and combustion properties of intumescing composites. Polym Degrad Stab. 2013;98:590–6.
10. Xuan S, Wang X, Song L, Xing W, Lu H, Hu Y. Study on flame-retardancy and thermal degradation behaviors of intumescent flame-retardant polylactide systems. Polym Int. 2011;60:1541–7.
11. Tao K, Li J, Xu L, Zhao X, Xue L, Fan X, Yan Q. A novel phosphazene cyclomatrix network polymer: design, synthesis and application in flame retardant polylactide. Polym Degrad Stab. 2011;96:1248–54.
12. Reti C, Casetta M, Duquesne S, Delobel R, Soulestin J, Bourbigot S. Intumescent biobased-polylactide films to flame retard nonwovens. J Eng Fibers Fabr. 2009;4:33–9.
13. Zhan J, Song L, Nie S, Hu Y. Combustion properties and thermal degradation behavior of polylactide with an effective intumescent flame retardant. Polym Degrad Stab. 2009;94:291–6.
14. Ye L, Ren J, Cai SY, Wang ZG, Li JB. Poly(lactic acid) nanocomposites with improved flame retardancy and impact strength by combining of phosphinates and organoclay. Chin J Polym Sci. 2016;34:785–96.
15. Wang DY, Leuteritz A, Wang YZ, Wagenknecht U, Heinrich G. Preparation and burning behaviors of flame retarding biodegradable poly(lactic acid) nanocomposite based on zinc

aluminum layered double hydroxide. Polym Degrad Stab. 2010;95:2474–80.
16. Fontaine G, Bourbigot S. Intumescent polylactide: a nonflammable material. J Appl Polym Sci. 2009;113:3860–5.
17. Tang G, Zhang R, Wang X, Wang B, Song L, Hu Y, Gong X. Enhancement of flame retardant performance of bio-based polylactic acid composites with the incorporation of aluminum hypophosphite and expanded graphite. J Macromol Sci Part A Pure Appl Chem. 2013;50:255–69.
18. Schartel B, Braun U, Schwarz U, Reinemann S. Fire retardancy of polypropylene/flax blends. Polymer. 2003;44:6241–6250.
19. Gallo E, Schartel B, Acierno D, Russo P. Flame retardant biocomposites: synergism between phosphinate and nanometric metal oxides. Eur Polym J. 2011;47:1390.
20. Kandola BK. Natural polymers. Volume 1: composites. Cambridge: The Royal Society of Chemistry; 2012. pp. 86–117.
21. Gallo E, Sánchez-Olivares G, Schartel B. Flame retardancy of starch–based biocomposites – aluminum hydroxide-coconut fiber synergy. Polimery 2013;58:395.
22. Gallo E, Schartel B, Acierno D, Cimino F, Russo P. Tailoring the flame retardant and mechanical performances of natural fiber-reinforced biopolymer by multi-component laminate. Compos Part B. 2013;44:112.
23. Suardana NPG, Ku MS, Lim JK. Effects of diammonium phosphate on the flammability and mechanical properties of biocomposites. Mater Design. 2011;32:1990.
24. Chen J, Zhang P, Zhang Y. Patent CN105219043-A, 2016.
25. Yang W, Jia Z, Chen Y, Zhang Y, Si J, Lu H, Yang B. Carbon nanotube reinforced polylactide/basalt fiber composites containing aluminium hypophosphite: thermal degradation, flame retardancy and mechanical properties. RSC Adv. 2015;5:105869.
26. Saba N, Jawaid M, Alothman OY, Inuwa IM, Hassan A. A review on potential development of flame retardant kenaf fibers reinforced polymer composites. Polym Adv Technol. 2017;28:424–34.
27. Shukor F, Hassan A, Islam MS, Mokhtar M, Hasan M. Effect of ammonium polyphosphate on flame retardancy, thermal stability and mechanical properties of alkali treated kenaf fiber filled PLA biocomposites. Mater Design. 2014;54:425–429.
28. Subasinghe A, Bhattacharyya D. Compos. Performance of different intumescent ammonium polyphosphate flame retardants in PP/kenaf fibre composites. Part Appl Sci Manufac. 2014;65:91.
29. Leisewitz A, Kruse H, Schramm E. Substituting Environmentally Relevant Flame Retardants: Assessment Fundamentals, Volume I: Results and summary overview, Commissioned by the German Federal Environmental Agency (Umweltbundesamt, UBA), 2000.
30. Zhang X, Guo F, Chen J, Wang G, Liu H. Investigation of interfacial modification for flame retardant ethylene vinyl acetate copolymer/alumina trihydrate nanocomposites. Polym Degrad Stab. 2005;87:411–8.
31. Hippi U, Mattila J, Korhonen M, Seppälä J. Compatibilization of polyethylene/aluminum hydroxide (PE/ATH) and polyethylene/magnesium hydroxide (PE/MH) composites with functionalized polyethylenes. Polymer 2003;44:1193–201.
32. Camino G, Maffezzoli A, Braglia M, De Lazzaro M, Zammarano M. Effect of hydroxides and hydroxycarbonate structure on fire retardant effectiveness and mechanical properties in ethylene-vinyl acetate copolymer. Polym Degrad Stab. 2001;74:457–64.
33. Hornsby PR, Watson CL. Interfacial modification of polypropylene composites filled with magnesium hydroxide. J Mater Sci. 1995;30:5347–55.
34. Gilman JW, Kashiwagi T, Lichtenhan JD. Nanocomposites: a revolutionary new flame retardant approach. SAMPE J. 1997;33:40–6.
35. Dittrich B, Wartig KA, Hofmann D, Mülhaupt R, Schartel B. The influence of layered, spherical, and tubular carbon nanomaterials' concentration on the flame retardancy of polypropylene. Polym Compos. 2015;36:1230–41.
36. Kashiwagi T, Du FM, Winey KI, Groth KA, Shields JR, Bellayer SP, Kim H, Douglas JF. Flammability properties of polymer nanocomposites with single-walled carbon nanotubes: effects of nanotube dispersion and concentration. Polymer 2005;46:471–81.
37. Bartholmai M, Schartel B. Layered silicate polymer nanocomposites: new approach or illusion for fire retardancy? Investigations of the potentials and the tasks using a model system. Polym Adv Technol. 2004;15:355–64.
38. Beyer G. Flame retardant properties of EVA-nanocomposites and improvements by combination of nanofillers with aluminium trihydrate. Fire Mater. 2001;25:193–7.
39. Haurie L, Fernandez AI, Velasco JI, Chimenos JM, Cuesta JM, Espiell F. Thermal stability and flame retardancy of LDPE/EVA blends filled with synthetic hydromagnesite/aluminium hydroxide/montmorillonite and magnesium hydroxide/aluminium hydroxide/montmorillonite mixtures. Polym Degrad Stab. 2007;92:1082–7.
40. Schartel B, Knoll U, Hartwig A, Pütz D. Phosphonium-modified layered silicate epoxy resins nanocomposites and their combinations with ATH and organo-phosphorus fire retardants. Polym Adv Technol. 2006;17:281–93.
41. Dittrich B, Wartig KA, Mülhaupt R, Schartel B. Flame-retardancy properties of intumescent ammonium poly(phosphate) and mineral filler magnesium hydroxide in combination with graphene. Polymers 2014;6:2875–95.
42. Camino G, Costa L, Trossarelli L. Study of the mechanism of intumescence in fire retardant polymers: Part V – Mechanism of formation of gaseous products in the thermal degradation of ammonium polyphosphate. Polym Degrad Stab. 1985;12:203–11.
43. Horrocks AR. Fire retardant materials. Cambridge: Woodhead Publishing Limited; 2001. pp. 128–81.
44. Green J. Fire retardancy of polymeric materials. New York: Marcel Dekker Inc.; 2000. pp. 147–70.
45. Zhu H, Zhu Q, Li J, Tao K, Xue L, Yan Q. Synergistic effect between expandable graphite and ammonium polyphosphate on flame retarded polylactide. Polym Degrad Stab. 2011;96:183–9.
46. Reimschuessel HK, Shalaby SW, Pearce EM, J. On the oxygen index of nylon 6. Fire Flammability. 1973;4:299–308.
47. Schartel B, Pötschke P, Knoll U, Abdel-Goad M. Fire behaviour of polyamide 6/multiwall carbon nanotube nanocomposites. Eur Polym J. 2005;41:1061–70.
48. Dittrich B, Wartig KA, Hofmann D, Mülhaupt R, Schartel B. Carbon black, multiwall carbon nanotubes, expanded graphite and functionalized graphene flame retarded polypropylene nanocomposites. Polym Adv Technol. 2013;24:916–26.
49. Schartel B, Braun U. Comprehensive fire behaviour assessment of polymeric materials based on cone calorimeter investigations. e-Polymers 2003;13.

50. Schartel B, Hull TR. Development of fire-retarded materials – Interpretation of cone calorimeter data. Fire Mater. 2007;31:327–54.
51. Hull TR, Stec AA, Nazare S. Fire retardant effects of polymer nanocomposites. J Nanosci Nanotechnol. 2009;9:4478–86.
52. Duquesne S, Le Bras M, Bourbigot S, Delobel R, Camino G, Eling B, Lindsay C, Roels T. Thermal degradation of polyurethane and polyurethane/expandable graphite coatings. Polym Degrad Stab. 2001;74:493–9.
53. Camino G. In: Fire retardancy of polymeric materials. New York: Marcel Dekker Inc.; 2000. pp. 217–43.
54. Schartel B, Bartholmai M, Knoll U. Some comments on the main fire retardancy mechanisms in polymer nanocomposites. Polym Adv Technol. 2006;17:772–7.